Szalai, R., Stépán, G., & Hogan, S. J. (2002). Global dynamics of low immersion high-speed milling.

Global dynamics of low immersion high-speed milling*

Róbert Szalai † Gábor Stépán ‡ S. John Hogan §

7th July 2004

Abstract

In the case of low immersion high-speed milling, the ratio of time spent cutting to not cutting can be considered as a small parameter. In this case the classical regenerative vibration model of machine tool vibrations reduces to a simplified discrete mathematical model. The corresponding stability charts contain stability boundaries related to period doubling and Neimark-Sacker bifurcations. The subcriticality of both types of bifurcations is proved in this paper. Further, global period-2 orbits are found and analyzed. In connection with these orbits, the existence of chaotic motion is demonstrated for realistic high-speed milling parameters.

High-speed milling is one of the most efficient cutting processes used in industry. In the process of optimizing this technology, it is a challenging task to understand its special dynamical properties. Although this field has a vast literature (e.g. [2, 1, 15, 4, 3, 10]), very little is known about the nonlinear dynamics of high-speed milling processes. In this paper we investigate a nonlinear discrete time model, whose linear counterpart was constructed first by Davies et al. [4]. This nonlinear model is simple enough to have closed form results, which qualitatively describe complicated phenomena found by simulations in a delay equation model of the process [3, 11]. Particularly, the stability analysis in Davies et al.[4] shows that the fixed point of the model can lose its stability in two ways: either by a Neimark-Sacker bifurcation or by a period doubling bifurcation. Here we prove that both bifurcations are subcritical. We also investigate another period-2 motion. This second period-2 motion corresponds to the tool cutting only every second period. Similarly, this motion can also bifurcate in the two ways mentioned above. In the case when the unstable

*PACS: 05.45.-a

†Department of Applied Mechanics, Budapest University of Technology and Economics, P.O. Box 91, H-1521, Budapest, Hungary, e-mail: szalai@mm.bme.hu

‡Department of Applied Mechanics, Budapest University of Technology and Economics, P.O. Box 91, H-1521, Budapest, Hungary, e-mail: stepan@mm.bme.hu

§Department of Engineering Mathematics, University of Bristol, BS8 1TR, Bristol, United Kingdom, e-mail: s.j.hogan@bristol.ac.uk

fixed point coexists with an unstable period two orbit chaos can arise, which is shown to be generic to the system.

1 Introduction

High-speed milling is a very common machining process in industry. It is specially used in the automotive and aerospace industry, due to its precision and effectiveness. It is particularly efficient at removing significant amount of material from a workpiece. In the case study by Halley et *al.* [9] it is shown that manufacturing of large, sculptured and thin walled parts, where 80-90% of the material is removed by cutting, can be more economical than producing a large number of simple parts. The reason for this is that the assembly and storage of parts can be heavily simplified compared to the traditional procedure and at the same time the cost of machining may be kept at a reasonable level using high-speed milling.

In milling processes cutting is done by a rotating tool, which has edges to remove material by inducing mainly shear stress in the workpiece. In general, the cutting tool can have very complicated geometry in order to obtain special surfaces or can be very large if the workpiece is intended to be cut in one turn. In contrast to general milling, high-speed milling has specific properties such as small tool diameter, low number of milling teeth (2, 3 or 4), and high cutting speed. Also, if the immersion is low the above features lead to so-called highly interrupted cutting. This means that, most of the time, none of the cutting edges is in contact with the workpiece, while cutting occurs during those short time-intervals only when one of the teeth hits the workpiece. Actually, the ratio of time spent cutting to not cutting may be less than 10%, so it can be considered as a small parameter.

Stability of machining processes was first studied by Tlusty [23] and Tobias [24], who showed that the so-called regenerative effect, where the force acting on the tool mainly depends on the difference of the current and a delayed tool position, plays an essential role in the dynamics of cutting. This observation generally yields delay equation models of tool motion and results the appearance of the lobe structure in stability charts. While constant speed turning processes are described by automonous delay equations, milling is time periodic and therefore its stability analysis is more involved. In the case of large or full immersion, these time-periodic equations may be analysed by harmonic balance techniques, which reduce the infinite dimensional problem to finite dimensions. As Davies et *al.* [4] pointed out, this is not a viable approach in case of the highly interrupted cutting due to high order harmonics content of impact like dynamics. They introduced a new and more simple model, which describes cutting as an impact that still involvesthe delay effect. Also, they gave experimental verification of the model. The nonlinear model we will analyse in this paper is the simplest way of incorporating the nonlinear cutting force function described by the three-quarter rule [23] into the linear model of Davies et *al.* [4].

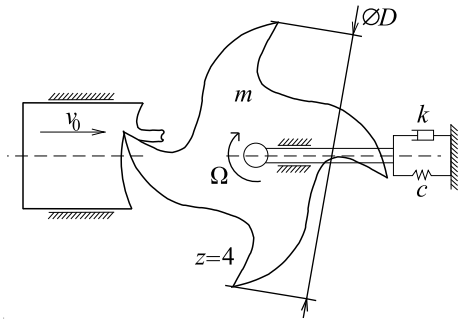

Figure 1: Scheme of high-spee milling. Feed is provided by the workpiece velocity v_0, cutting speed is provided by the (rotating) tool.

Early results on nonlinear dynamics of turning processes [18] show that cutting just below the stability boundary is sensitive to perturbations, so that stable cutting can suddenly turn into chatter. An analytical investigation of Stépán and Kalmár-Nagy[19] (see also Kalmár-Nagy et *al.* [12]) has revealed that this phenomenon is related to a subcritical Hopf bifurcation in the delay equation model. In the case of milling there are two ways of losing stability, which are the classical Hopf-type (Neimark-Sacker) and period doubling bifurcation, which is analysed by several authors including Insperger et *al.* [10], Bayly et *al.* [3]. The nonlinear dynamics is mostly studied by simulation (for an overview see Balachandran [2]), but in several cases subcriticality is not observed due to linear cutting force functions. However these simulations [2] together with experiments [14] show that the loss of stability by period doubling yields a sudden transition to stable period-2 vibrations or chaotic motion, which indicate that the bifurcation is most likely subcritical. Hence, there is a need for a nonlinear cutting force function.

The outline of the paper is as follows. In the section 2 we introduce the nonlinear governing equation of the process, which will be simplified to a discrete system in section 3. Section 4 contains basic stability information [4] adapted to our nonlinear model. In section 5 the period doubling and Neimark-Sacker bifurcations occuring at the stability boundaries are analysed and their subcriticality is proved. Existence, stability and bifurcations of a "global" period-2 orbits are discussed in section 6. Finally, chaos is demonstrated for parameters, where the steady state motion and the added period-2 motions are both unstable.

2 Mechanical model

We use the simplest possible mechanical model of the process. The tool is modeled as a 1 degree of freedom (DOF) oscillator with undamped natural (angular) frequency $\omega_n = \sqrt{c/m}$, relative damping factor $\zeta = k/(2m\omega_n)$, and

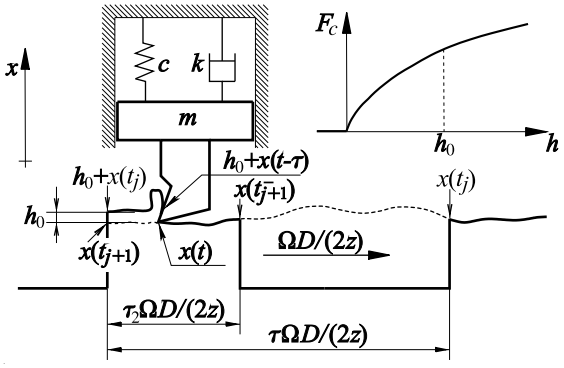

Figure 2: Mechanical model. Note the difference from the model in Fig. 1: the feed is provided by the tool while the cutting speed is provided by the motion of the (rotating) workpiece.

damped natural frequency $\omega_d = \omega_n\sqrt{1-\zeta^2}$, where c is the stiffness and k denotes the damping factor. The tool rotates with the constant angular speed Ω and has z number of edges. In the case of low immersion high-speed milling, the tool cuts only during a small fragment of the cutting period, so in Fig. 1, the workpiece is considered to be thin in the cutting direction and cutting can be approximated as an impact.

Consequently the motion of the tool can be separated into two parts. As it can be seen in Fig. 2, the tool oscillates freely for time period $\tau_1 = \tau - \tau_2$ and then cuts the workpiece for time period τ_2. The tool starts the free vibration at time instants $t_j = t_0 + j\tau$, $j \in \mathbb{Z}$, enters the workpiece at $t_{j+1}^- = t_{j+1} - \tau_2$ and finishes cutting at t_{j+1} when it starts free-flight, again. For the entire dynamics, we have the equation of motion

$$\ddot{x}(t) + 2\zeta\omega_n\dot{x}(t) + \omega_n^2 x(t) = \frac{g(t)}{m}F_c(h(t)), \tag{1}$$

where

$$g(t) = \begin{cases} 0 & \text{if} \quad \exists\, j \in \mathbb{Z}: \quad t_j \leqslant t < t_{j+1}^- \\ 1 & \text{if} \quad \exists\, j \in \mathbb{Z}: \quad t_{j+1}^- \leqslant t < t_{j+1} \end{cases}.$$

The cutting force F_c, in general, may depend on many factors of the process like cutting speed, lubrication, etc.. In our model, we consider its dependence merely on geometrical data, namely on the constant chip width w and on the time-varying chip thickness $h(t)$ in the form of the empirical three-quarter rule [23]

$$F_c(h(t)) = Kw(h(t))^{3/4}, \tag{2}$$

where K is an experimentally determined parameter. The chip thickness is computed from the current and a delayed tool tip position, i.e.,

$$h(t) = h_0 + x(t-\tau) - x(t),$$

where $h_0 = v_0\tau$ is the feed for a cutting period (see Fig. 1).

Introducing the dimensionless time $\hat{t} = \omega_n t$, the governing equation (1) becomes

$$\ddot{x}(\hat{t}) + 2\zeta\dot{x}(\hat{t}) + x(\hat{t}) = g(\hat{t})\frac{Kw}{m\omega_n^2}(h_0 + x(\hat{t}-\hat{\tau}) - x(\hat{t}))^{3/4}.$$

In what follows by abuse of notation we drop the hat from the dimensionless time variables $\hat{t}$, $\hat{\tau}$, $\hat{\tau}_1$, $\hat{\tau}_2$. For the free-flight period ($g(t) \equiv 0$) we have

$$\ddot{x}(t) + 2\zeta\dot{x}(t) + x(t) = 0 \qquad t_j^- \leqslant t < t_j,$$

which can be solved and arranged in discrete form:

$$\begin{pmatrix} x(t_{j+1}^-) \\ \dot{x}(t_{j+1}^-) \end{pmatrix} = A \begin{pmatrix} x(t_j) \\ \dot{x}(t_j) \end{pmatrix}. \tag{3}$$

When the time period of cutting is very short, i.e., $\tau_2 \to 0$ then the time period τ_1 of the free-flight can be approximated by the tooth-pass period τ. In this way the coefficient matrix A constructed from the linear solution of the free-flight assumes the form

$$A = \begin{pmatrix} \mathrm{e}^{-\zeta\tau}\left(\cos(\hat{\omega}_d\tau) + \frac{\zeta}{\hat{\omega}_d}\sin(\hat{\omega}_d\tau)\right) & \frac{\mathrm{e}^{-\zeta\tau}}{\hat{\omega}_d}\sin(\hat{\omega}_d\tau) \\ -\frac{\mathrm{e}^{-\zeta\tau}}{\hat{\omega}_d}\sin(\hat{\omega}_d\tau) & \mathrm{e}^{-\zeta\tau}\left(\cos(\hat{\omega}_d\tau) - \frac{\zeta}{\hat{\omega}_d}\sin(\hat{\omega}_d\tau)\right) \end{pmatrix}, \tag{4}$$

where the dimensionless damped natural frequency is

$$\hat{\omega}_d = \omega_d/\omega_n = \sqrt{1-\zeta^2}.$$

For the cutting period $\tau_2 \to 0$, we neglect all the forces (spring, damping) except the cutting force, and assume that the position of the tool does not change much during the impact

$$\ddot{x}(t) \approx \frac{Kw}{m\omega_n^2}(h_0 + x(t_j) - x(t_{j+1}^-))^{3/4}, \qquad t_{j+1}^- \leqslant t < t_{j+1}.$$

Integrating the above formula on $[t_{j+1}^-, t_{j+1}]$ we find

$$\dot{x}(t_{j+1}) = \dot{x}(t_{j+1}^-) + \tau_2\frac{Kw}{m\omega_n^2}(h_0 + x(t_j) - x(t_{j+1}^-))^{3/4}. \tag{5}$$

Putting together equations (3) and (5) yields

$$\begin{aligned} x(t_{j+1}) &= A_{11}x(t_j) + A_{12}\dot{x}(t_j) \\ \dot{x}(t_{j+1}) &= A_{21}x(t_j) + A_{22}\dot{x}(t_j) + \frac{Kw\tau_2}{m\omega_n^2}\left(h_0 + (1-A_{11})x(t_j) - A_{12}\dot{x}(t_j)\right)^{3/4}, \end{aligned}$$

where A_{ij} denote the corresponding elements of A in (4).

3 Nonlinear discrete map

In the previous section, we constructed the equations mapping the state of system from cutting period to subsequent cutting period. We rephrase it with the state variables $x_j = x(t_j)$ and $v_j = \dot{x}(t_j)$, so the map becomes

$$\begin{pmatrix} x_{j+1} \\ v_{j+1} \end{pmatrix} = A \begin{pmatrix} x_j \\ v_j \end{pmatrix} + \begin{pmatrix} 0 \\ \frac{Kw\tau_2}{m\omega_n^2} \left(h_0 + (1 - A_{11})x_j - A_{12}v_j\right)^{3/4} \end{pmatrix}. \tag{6}$$

This map has a fixed point

$$\begin{pmatrix} x_e \\ v_e \end{pmatrix} = \frac{Kw\tau_2 h_0^{3/4}}{m\omega_n^2(1 + \det A - \mathrm{tr}A)} \begin{pmatrix} A_{12} \\ 1 - A_{11} \end{pmatrix} \tag{7}$$

that corresponds to stationary cutting, which is a period-1 motion with period τ. Linearizing around this fixed point, we get the local dynamics

$$\begin{pmatrix} x_{j+1} \\ v_{j+1} \end{pmatrix} = \begin{pmatrix} x_e \\ v_e \end{pmatrix} + B \begin{pmatrix} x_j \\ v_j \end{pmatrix}, \qquad B = \begin{pmatrix} A_{11} & A_{12} \\ A_{21} + \hat{w}(1 - A_{11}) & A_{22} - \hat{w}A_{12} \end{pmatrix}, \tag{8}$$

where the dimensionless chip width

$$\hat{w} = \frac{3}{4h_0^{1/4}} \frac{K\tau_2}{m\omega_n^2} w$$

is assumed later as the bifurcation parameter. Note, that in the limiting case of $\tau_2 \to 0$ and $\tau_1 \to \tau$, the original chip width w tends to infinity at finite $\hat{w}$, which means that the extremely (highly) interrupted cutting could theoretically take place with infinite chip width.

4 Stability chart

This section summarizes the linear stability results of [4]. In our model (6) only flip or Neimark-Sacker bifurcation can occur. For the flip case we have a characteristic multiplier at -1, that is

$$\det(B(\hat{w}_{\mathrm{cr}}^{\mathrm{f}}) + I) = 0.$$

This equation can be solved for $\hat{w}$ in the form

$$\hat{w}_{\mathrm{cr}}^{\mathrm{f}} = \frac{\det A + \mathrm{tr}A + 1}{2A_{12}} = \hat{\omega}_d \frac{\cos(\hat{\omega}_d\tau) + \cosh(\zeta\tau)}{\sin(\hat{\omega}_d\tau)}. \tag{9}$$

For the Neimark-Sacker case we have

$$\det B(\hat{w}_{\mathrm{cr}}^{\mathrm{ns}}) = 1,$$

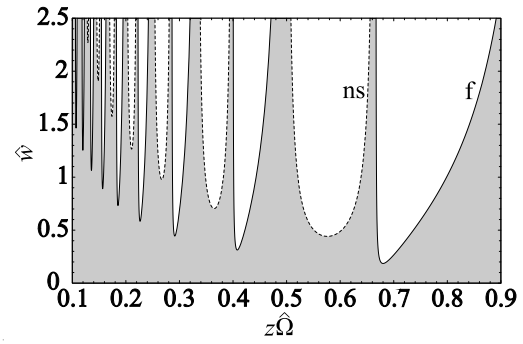

Figure 3: Stability chart. Grey regions are stable, continuous lines denote period doubling boundaries while dashed lines correspond to Neimark-Sacker bifurcation

because B is real and its complex eigenvalues are conjugate pairs. Solving this equation for $\hat{w}$ yields

$$\hat{w}_{\mathrm{cr}}^{\mathrm{ns}} = \frac{\det A - 1}{A_{12}} = -2\hat{\omega}_d \frac{\sinh(\zeta\tau)}{\sin(\hat{\omega}_d\tau)}. \tag{10}$$

The results are shown in Figure 3. This so-called stability chart is constructed in the plane of the most important technological parameters. One of these is the cutting speed represented by the product $z\hat{\Omega} = 2\pi/\tau$ of the number z of cutting edges and dimensionless angular speed $\hat{\Omega}$, while the other parameter is the dimensionless chip width $\hat{w}$.

5 Local bifurcations

In this section, we show that bifurcations occuring at stability boundaries (9) and (10) are both subcritical. In order to do this, we use standard techniques of local bifurcation theory, which can be found, for example, in [8]. To apply these techniques, we need the Taylor expansion of this map (6) at its fixed point (7). This requires the expansion of the cutting force function F_c in (2) at theoretical chip thickness h_0 with respect to the chip thickness variation Δh

$$F_c(h_0 + \Delta h) \approx K w h_0^{3/4} + \frac{3Kw}{4h_0^{1/4}}\Delta h - \frac{3Kw}{32h_0^{5/4}}(\Delta h)^2 + \frac{5Kw}{128h_0^{9/4}}(\Delta h)^3$$

or with the dimensionless chip width $\hat{w}$

$$F_c(h_0 + \Delta h)\frac{\tau_2}{m\omega_n^2} \approx \frac{4\hat{w}}{3}h_0 + \hat{w}\Delta h - \frac{\hat{w}}{8h_0}(\Delta h)^2 + \frac{5\hat{w}}{96h_0^2}(\Delta h)^3.$$

In what follows, we consider $\hat{w}$ as the bifurcation parameter, thus the system around the fixed point is now approximated by

$$\begin{pmatrix} x_{j+1} \\ v_{j+1} \end{pmatrix} = \begin{pmatrix} x_e \\ v_e \end{pmatrix} + B(\hat{w}) \begin{pmatrix} x_j \\ v_j \end{pmatrix} + \begin{pmatrix} 0 \\ \hat{w} \sum_{q+r=2,3} b_{qr} x_j^q v_j^r \end{pmatrix}, \tag{11}$$

where

$$b_{20} = -\frac{(1-A_{11})^2}{8h_0}, \quad b_{11} = \frac{(1-A_{11})A_{12}}{4h_0}, \quad b_{02} = -\frac{A_{12}^2}{8h_0},$$
$$b_{30} = \frac{5(1-A_{11})^3}{96h_0^2}, \quad b_{21} = -\frac{5(1-A_{11})^2 A_{12}}{32h_0^2},$$
$$b_{12} = \frac{5(1-A_{11})A_{12}^2}{32h_0^2}, \quad b_{03} = -\frac{5A_{12}^3}{96h_0^2}.$$

5.1 Flip bifurcation

Crossing the stability boundaries at (9) a flip bifurcation occurs. At the stability boundaries the critical eigenvalue is

$$\lambda_1(\hat{w}_{\mathrm{cr}}^{\mathrm{f}}) = -1$$

and the linear part of the system (11) can be written as

$$T^{-1} B(\hat{w}_{\mathrm{cr}}^{\mathrm{f}}) T = \begin{pmatrix} -1 & 0 \\ 0 & \lambda_2 \end{pmatrix},$$

where T is a transformation matrix and contains the eigenvectors $s_{1,2}$ of $B(\hat{w}_{\mathrm{cr}}^{\mathrm{f}})$, i.e.,

$$T := (s_1, s_2) = \begin{pmatrix} 1 & 1 \\ -\zeta - \frac{-\hat{\omega}_d\left(e^{\zeta\tau} + \cos(\hat{\omega}_d\tau)\right)}{\sin(\hat{\omega}_d\tau)} & -\zeta + \frac{-\hat{\omega}_d \sinh(\zeta\tau)}{\sin(\hat{\omega}_d\tau)} \end{pmatrix}$$

and

$$\lambda_2(\hat{w}_{\mathrm{cr}}^{\mathrm{f}}) = \mathrm{e}^{-\zeta\tau} \left(\cos(\hat{\omega}_d\tau) + \sinh(\zeta\tau)\right). \tag{12}$$

We do a local analysis in the neighborhood of $X_{\mathrm{cr}}^{\mathrm{f}} = ((x_e, v_e), \hat{w}_{\mathrm{cr}}^{\mathrm{f}}) \in \mathbb{R}^2 \times \mathbb{R}$. We consider the following perturbation of the system (11) around $X_{\mathrm{cr}}^{\mathrm{f}}$ in the coordinate system of the eigenvectors of $B(\hat{w}_{\mathrm{cr}}^{\mathrm{f}})$

$$\begin{pmatrix} \xi_{j+1} \\ \eta_{j+1} \end{pmatrix} = \begin{pmatrix} -1 + a^{\mathrm{f}} \Delta\hat{w} & 0 \\ 0 & C_{22} \end{pmatrix} \begin{pmatrix} \xi_j \\ \eta_j \end{pmatrix} + \begin{pmatrix} \sum_{q+r=2,3} c_{qr} \xi_j^q \eta_j^r \\ \sum_{q+r=2,3} d_{qr} \xi_j^q \eta_j^r \end{pmatrix}, \tag{13}$$

where a^{f} is the derivative of $\lambda_1(\hat{w})$ at $\hat{w}_{\mathrm{cr}}^{\mathrm{f}}$

$$a^{\mathrm{f}} = \left.\frac{\partial\lambda_1}{\partial\hat{w}}\right|_{\hat{w}_{\mathrm{cr}}^{\mathrm{f}}} = -\frac{2}{\hat{\omega}_d} \frac{\sin(\hat{\omega}_d\tau)}{\cos(\hat{\omega}_d\tau) + \cosh(\zeta\tau) + 2\sinh(\zeta\tau)} < 0$$

and the nonlinear coefficients c_{qr}, d_{qr} are computed from b_{qr} with the help of the transformation matrix T.

From the center manifold theorem we know that there exists an invariant manifold containing $X_{\rm cr}^{\rm f}$ that is tangent to the eigenvector corresponding to the critical eigenvalue -1. In the present case, the center manifold is attracting since $|\lambda_2| < 1$ in (12) and its graph can be written in the power series [20]

$$\xi \mapsto \mathrm{col}(\xi, h(\xi)), \quad h(\xi) = h_2\xi^2 + \ldots, \quad h_2 = \frac{d_{20}}{1-\lambda_2}.$$

The projection of (13) into the center manifold gives the scalar nonlinear map

$$\xi_{j+1} = (-1 + a^{\rm f}\Delta\hat{w})\xi_j + c_{20}\xi_j^2 + (c_{30} + \frac{c_{11}d_{20}}{1-\lambda_2})\xi_j^3 + \cdots . \tag{14}$$

We seek period-2 orbits that arise in the neighborhood of the fixed point, therefore consider the second iterate of (14) having the form

$$\xi_{j+2} = (1 - 2a^{\rm f}\Delta\hat{w})\xi_j - 2\delta\xi_j^3 + \cdots , \tag{15}$$

where

$$\delta = c_{20}^2 + c_{30} + \frac{c_{11}d_{20}}{1-\lambda_2}.$$

The period-2 points on the center manifold can be found as the fixed point of (15), namely

$$\xi_{1,2} = \pm\sqrt{-\frac{a^{\rm f}\Delta\hat{w}}{\delta}}.$$

Thus, the sense of the flip bifurcation is determined by the sign of δ. A tedious algebraic calculation yields

$$\delta = -\frac{5}{12h_0^2}\frac{\cosh(\zeta\tau) + \cos(\hat{\omega}_d\tau)}{\cosh(\zeta\tau) + 2\sinh(\zeta\tau) + \cos(\hat{\omega}_d\tau)} < 0,$$

which shows that the arising bifurcation is always subcritical. Unstable period-2 motions exist around the stable fixed point near the stability boundary.

The simulation in Fig. 4 shows the saddle type period-2 motion represented by $(\xi_1, h(\xi_1))$ and $(\xi_2, h(\xi_2))$. The basin of attraction of the stable fixed point (x_e, v_e) is approximated by the two straight lines parallel to s_2. Starting an iteration at (x_0, v_0) from between these parallel lines it converges to the fixed point. It can be seen that the rate of the convergence in the coordinate direction η is very fast, while in the orientation reversing direction ξ is very slow since the corresponding multiplier is slightly greater than -1.

5.2 Neimark-Sacker bifurcation

Along the stability boundaries (10), a Neimark-Sacker (also called secondary Hopf) bifurcation occurs, which can be related to the Hopf bifurcation of turning processes. At this type of bifurcation quasiperiodic orbits arise, which are living

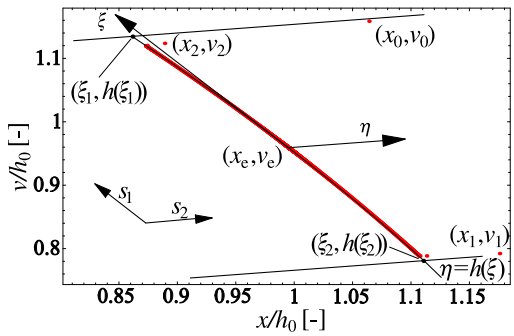

Figure 4: Simulation and analytical results for eq. (6) ($\hat{w} = 0.827$, $z\hat{\Omega} = 0.78$)

on an invariant closed curve about the fixed point in the case of a discrete system, or on an invariant 2 dimensional torus in the case of a vector field. The sense of the bifurcation, i.e. whether stable or unstable motion arise, can be calculated using the normal form reduction [8]. For the sake of simplicity we use complex transformation here. With the help of the complex eigenvectors $s_{1,2}$ belonging to the critical eigenvalues of $B(\hat{w}_{\rm cr}^{\rm ns})$

$$\lambda_{1,2} = \mathrm{e}^{\pm i\phi}, \quad \phi = \cos^{-1}\frac{\mathrm{tr}B}{2},$$

we construct the complex transformation matrix $T = (s_1, s_2)$ in the form

$$T = \begin{pmatrix} 1 & 1 \\ -\zeta - \hat{\omega}_d \cot(\hat{\omega}_d\tau) + \frac{\hat{\omega}_d \mathrm{e}^{\zeta\tau + i\phi}}{\sin(\hat{\omega}_d\tau)} & -\zeta - \hat{\omega}_d \cot(\hat{\omega}_d\tau) + \frac{\hat{\omega}_d \mathrm{e}^{\zeta\tau - i\phi}}{\sin(\hat{\omega}_d\tau)} \end{pmatrix}.$$

Similar to the flip case, the following approximation of the system (11) can be derived at $X_{\rm cr}^{\rm ns} = ((x_e, v_e), \hat{w}_{\rm cr}^{\rm ns}) \in \mathbb{R}^2 \times \mathbb{R}$ in the coordinate system of the above critical eigenvectors of $B(\hat{w}_{\rm cr}^{\rm ns})$

$$\begin{pmatrix} z_{j+1} \\ \bar{z}_{j+1} \end{pmatrix} = (1 + a^{\rm ns}\Delta\hat{w}) \begin{pmatrix} \mathrm{e}^{i\phi} & 0 \\ 0 & \mathrm{e}^{-i\phi} \end{pmatrix} \begin{pmatrix} z_j \\ \bar{z}_j \end{pmatrix} + \begin{pmatrix} \sum_{q+r=2,3} c_{qr} z_j^q \bar{z}_j^r \\ \sum_{q+r=2,3} d_{qr} z_j^q \bar{z}_j^r \end{pmatrix}, \tag{16}$$

where

$$a^{\rm ns} = \left.\frac{\partial|\lambda_{1,2}|}{\partial\hat{w}}\right|_{\hat{w}_{\rm cr}^{\rm ns}} = \frac{\partial}{\partial\hat{w}}\sqrt{\det B(\hat{w}_{\rm cr}^{\rm ns})} = -\frac{1}{2\hat{\omega}_d}\mathrm{e}^{-\zeta\tau}\sin(\hat{\omega}_d\tau) > 0.$$

We can transform out all $2^{\rm nd}$ degree terms from (16), but for the $3^{\rm rd}$ degree terms we have the resonance related to $\lambda_1 = \lambda_1^2\lambda_2$ and $\lambda_2 = \lambda_1\lambda_2^2$. Thus the normal form yields

$$\begin{pmatrix} z_{j+1} \\ \bar{z}_{j+1} \end{pmatrix} = \begin{pmatrix} \mathrm{e}^{i\phi} & 0 \\ 0 & \mathrm{e}^{-i\phi} \end{pmatrix} \begin{pmatrix} z_j \\ \bar{z}_j \end{pmatrix} + \begin{pmatrix} e_{21} z_j^2 \bar{z}_j \\ f_{12} z_j \bar{z}_j^2 \end{pmatrix}, \tag{17}$$

where

$$e_{21} = \overline{f_{12}} = 2\frac{c_{20}c_{11}}{1-\mathrm{e}^{i\phi}} + \frac{c_{11}\overline{c_{11}}}{1-\mathrm{e}^{-i\phi}} + \frac{c_{11}c_{20}}{\mathrm{e}^{2i\phi}-\mathrm{e}^{i\phi}} + 2\frac{c_{02}\overline{c_{02}}}{\mathrm{e}^{2i\phi}-\mathrm{e}^{-i\phi}} + c_{21}.$$

By multiplying the two coordinates of (17) and using $|z|^2 = z\bar{z}$ we transform (17) into

$$|z|^2 \mapsto (1+a^{\mathrm{ns}}\Delta\hat{w})^2|z|^2 + 2(1+a^{\mathrm{ns}}\Delta\hat{w})\delta|z|^4 + e_{21}f_{12}|z|^6,$$

where

$$\delta = \frac{1}{2}(e_{21}e^{-i\phi} + f_{12}e^{i\phi}) = \mathrm{Re}(e_{21}e^{-i\phi}).$$

Neglecting the 6^{th} degree term the solution for the radius $|z|$ of the invariant circle assumes the form

$$|z| = \sqrt{-\frac{2a^{\mathrm{ns}}\Delta\hat{w} + (a^{\mathrm{ns}})^2\Delta\hat{w}^2}{2(1+a^{\mathrm{ns}}\Delta\hat{w})\delta}} \approx \sqrt{-\frac{a^{\mathrm{ns}}\Delta\hat{w}}{\delta}}.$$

This circle in the discrete space of (x_j, v_j) corresponds to a quasiperiodic oscillation of our original mechanical structure during the milling process.

After a long algebraic calculation we obtain

$$\delta = \frac{\mathrm{e}^{-5\zeta\tau}\left(4\mathrm{e}^{4\zeta\tau} - 3\mathrm{e}^{2\zeta\tau} - 1\right)\left(\cosh(\zeta\tau) - \cos(\hat{\omega}_d\tau)\right)}{32h_0^2} > 0.$$

Since δ is always positive, we can conclude that the Neimark-Sacker bifurcation is subcritical, too. The consequence for the machining process is similar to the flip case: the basin of attraction of the stationary cutting is inside of an invariant ellipse in the phase space. Thus, if we perturb the system such that we leave the basin of attraction, the system starts large amplitude (initially quasiperiodic) vibrations. This is called chatter.

The dotted simulations in Fig. 5 diverge from the invariant ellipse (continuous line) and its approximated counterpart (dashed line), which represents the unstable quasiperiodic oscillation. We used the inverse map in the simulation to visualize this invariant unstable ellipse.

6 Period two motion with 'fly-overs'

In the previous sections we have shown that there is only one fixed point (stationary cutting) of the system and if it undergoes a period doubling bifurcation, the resulting orbits may reach the boundary, where the actual chip thickness h becomes negative, the tool misses the workpiece and the cutting force vanishes (see Fig. 2). Hence, we suspect that the corresponding orbits continue beyond this boundary. In order to find these orbits we must modify the governing equations in a way that the tool flies over the workpiece in every second period. The

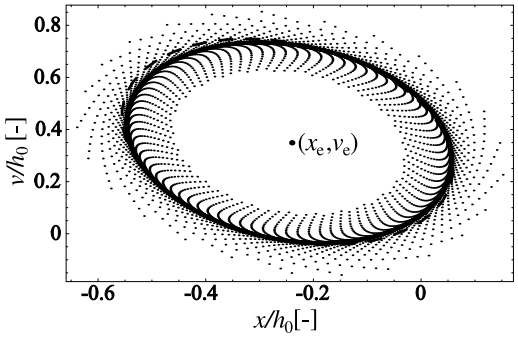

Figure 5: Simulation showing the computed (dashed line) and true repelling invariant manifold. ($\hat{w} = 0.503$, $z\hat{\Omega} = 0.55$)

equation for this motion will contain 2 times longer free-flights and impacts with the workpiece with double feed ($2h_0$). Thus, the governing equations become

$$\begin{pmatrix} x_{j+2} \\ v_{j+2} \end{pmatrix} = A^+ \begin{pmatrix} x_j \\ v_j \end{pmatrix} + \begin{pmatrix} 0 \\ \frac{Kw\tau_2}{m\omega_n^2}\left(2h_0 + (1 - A_{11}^+)x_j - A_{12}^+ v_j\right)^{3/4} \end{pmatrix}, \quad (18)$$

where $A^+ = A^2$ and A_{ij}^+ are the elements of A^+. Note, that A^+ can be obtained from A in (4) if 2τ is substituted instead of τ. This equation has a unique fixed point, again, but this time it physically corresponds to a period-2 motion

$$\begin{pmatrix} x_e^+ \\ v_e^+ \end{pmatrix} = \frac{Kw\tau_2(2h_0)^{3/4}}{m\omega_n^2(1 + \det A^+ - \mathrm{tr}A^+)} \begin{pmatrix} A_{12}^+ \\ 1 - A_{11}^+ \end{pmatrix}.$$

As explained above, this period-2 motion exists if the tool does not hit the workpiece after the first period of free-flight. This condition can be checked by the following equation based on the argument of the nonlinear term in (6)

$$0 > h(t_{j+1}^-) = h_0 + (1 - A_{11})x_e^+ - A_{12}v_e^+ = h_0 + \frac{Kw\tau_2}{m\omega_n^2}(2h_0)^{3/4}\left(\frac{(1 - A_{11})A_{12}^+ - (1 - A_{11}^+)A_{12}}{1 + \det A^+ - \mathrm{tr}A^+}\right). \quad (19)$$

After substituting the matrix elements and the dimensionless parameters we are left with

$$\hat{w} > \frac{3\hat{\omega}_d}{2^{7/4}} \frac{\cos(\hat{\omega}_d\tau) + \cosh(\zeta\tau)}{\sin(\hat{\omega}_d\tau)}. \quad (20)$$

Because of the similarity of the governing equations (6) and (18) the stability boundaries of (x_e^+, v_e^+) can be obtained from the same calculation just by changing the matrix A to A^+ and h_0 to $2h_0$. With the dimensionless parameters this calculation gives the stability boundaries of the period-2 motion in the form

$$\hat{w}_{\mathrm{cr}}^{f+} = 2^{1/4}\frac{\det A^+ + \mathrm{tr}A^+ + 1}{2A_{12}^+} = 2^{1/4}\omega_d \frac{\cos(2\omega_d\tau_1) + \cosh(2\zeta\tau_1)}{\sin(2\omega_d\tau_1)} \quad (21)$$

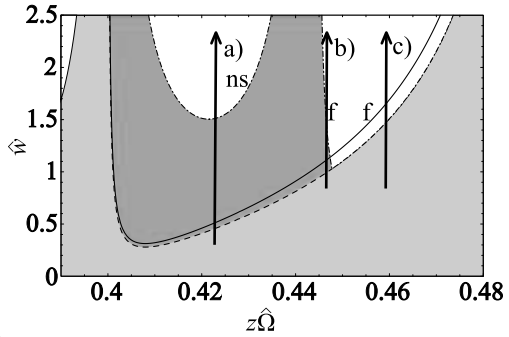

Figure 6: Global period-2 motions and their stability

and

$$\hat{w}_{\rm cr}^{\rm ns+} = 2^{1/4}\frac{\det A^+ - 1}{A_{12}^+} = -2^{7/4}\omega_d\frac{\sinh(2\zeta\tau_1)}{\sin(2\omega_d\tau_1)}. \tag{22}$$

A characteristic region of the corresponding stability chart is shown in Fig. 6. The stationary cutting (x_e, v_e) exists for all the parameters, it is stable below the continuous line representing a flip lobe of the stability chart in Fig. 3, and it is unstable above it. The period-2 motion (x_e^+, v_e^+) exists above the dashed line according to formula (20). In the light gray region only the stationary cutting exists and it is stable. The dash-dotted line "ns" refers to a stability boundary (22) of the period-2 motion, where Neimark-Sacker bifurcation occurs, while the dash-dotted line "f" refers to the other stability limit (21) where the period-2 motion undergoes another flip bifurcation. Thus, the dark gray region represents parameters, where stable period-2 motion exists, while in the white regions the outer period-2 motion is unstable.

To represent the above explained properties of the stability chart in Fig. 6, bifurcation diagrams are drawn for the parameter cases a), b), c) in Fig. 7. The unstable period doubling branches are computed using AUTO [5] that followed our analytic predictions perfectly. These computations also show that the inner and outer period-2 orbits are connected through a degenerate fold bifurcation, which means that orbits does not change smoothly by varying parameters and their characteristic multipliers are not even continous.

7 Chaotic oscillation

As we have seen in the bifurcation diagrams in Fig. 7, there are parameter regions where chaotic motions arise in the system. In this section, we investigate the simplest chaotic case, where both the fixed point and the outer period-2 orbit are unstable for case c) and $\hat{w} > \hat{w}_{\rm cr}^{\rm f}$. Both of the corresponding periodic points $((x_e, v_e),\ (x_e^+, v_e^+))$ are saddle-like, each has an unstable orientation reversing subspace as well as a stable orientation preserving subspace. Unfortunately, the

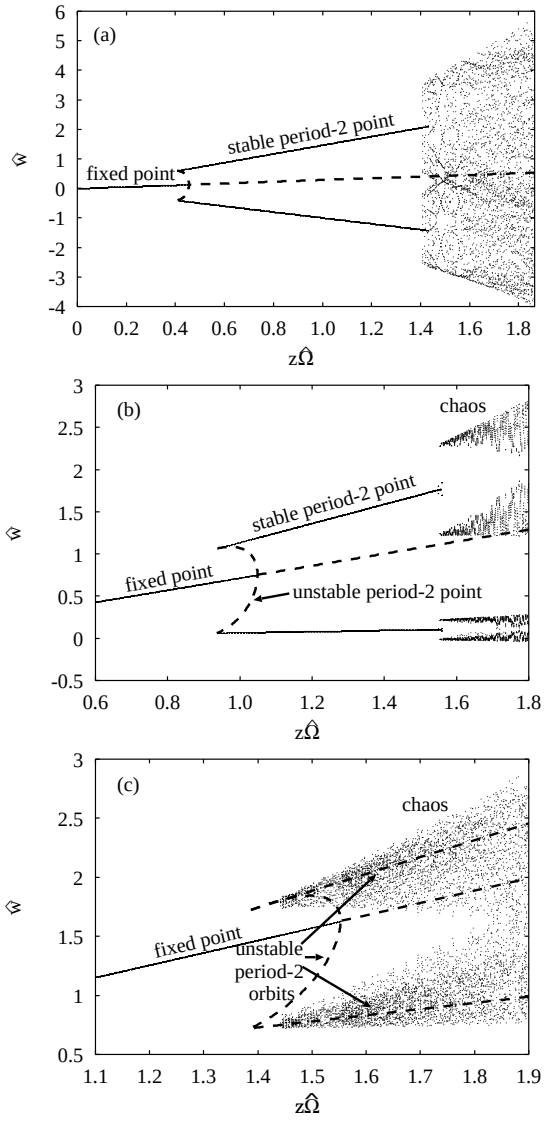

Figure 7: Bifurcation diagrams for cases a), b), c) in Fig. 6. The outer period-2 solution is stable and undergoes a Neimark-Sacker bifurcation (a) or a flip bifurcation (b). The period-2 solution is unstable, which induces chaotic motions around it (c).

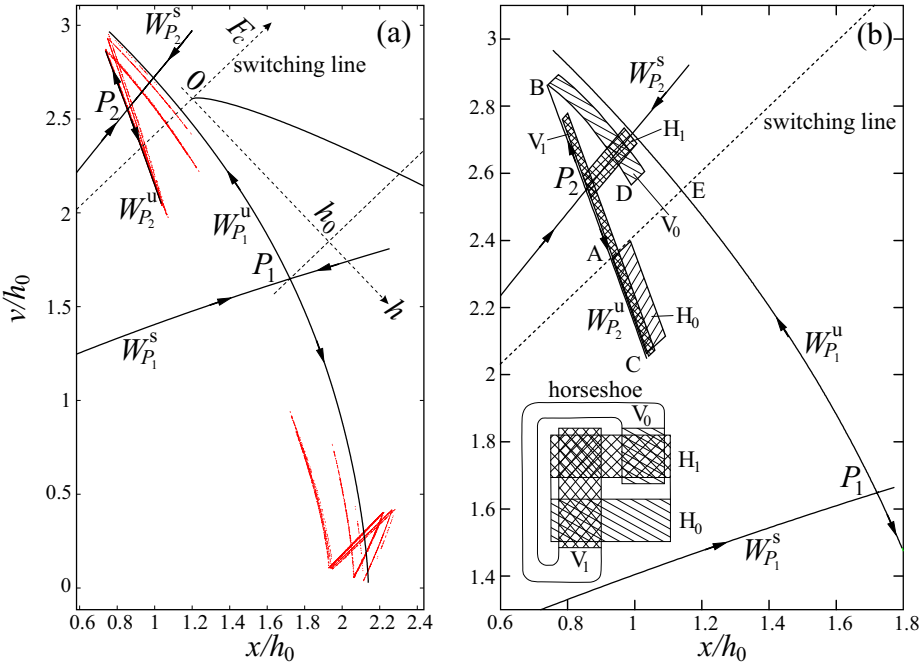

Figure 8: The chaotic map ($z\hat{\Omega} = 0.459$, $\hat{w} = 1.64$); a) simulation with invariant manifolds and how cutting force varies perpendicular to the switching line; b) horizontal and vertical slabs (see in the text).

local invariant manifolds are not to be extended to global manifolds because of the piecewise structure of the system, consequently, we have just global invariant sets, which are the union of images (preimages) of the local unstable (stable) manifold of the periodic points.

In Fig. 8.a the phase plane is presented for $\hat{w} = 1.64$. $P_1 = (x_e, v_e)$ is the fixed point representing stationary cutting, $P_2 = (x_e^+, v_e^+)$ refers to the period-2 motion. The invariant manifolds $W^{s,u}_{P_{1,2}}$ of these saddle points were computed using the software dstool module of J. England et *al.* [6]. The two parts of the dynamics are separated by the switching line $h(t^-_{j+1}) = 0$ in (19), where the cutting force F_c is nonsmooth. The cutting force characteristic of Fig. 2 is projected onto this plane to visualize the locations of the switching line and the fixed point P_1, where the chip thickness is 0 and h_0, respectively. The figure also shows simulation of a chaotic iteration. Below the switching line, we iterate equation (6), above that, (18). Since (18) describes every second τ-period, we use matrix A to produce the system's state in the middle of the period-2 free-flight. These additional iterated points show up among other points in the lower part of the figure, below $W^s_{P_1}$.

Demonstrating the proof of chaos, we use a geometric method in [25, 17]. In

fact, our system is conjugate to a modified version of Smale's horseshoe map. The construction of the map can be seen in Fig. 8.b. Let the map f be defined on this phase plane by (18) above the switching line and by every second iterate of (6) otherwise. Point A is defined as the intersection of $W^u_{P_2}$ and the switching line, then $B := f(A)$, $C := f(B)$, $D := f(C)$. Note A is part of both dynamics and as the entire switching line will be mapped by (18) and by that second iterate of (6) to the same place. Further, let E be the intersection of $W^u_{P_1}$ and the switching line. According to numerical results, the stable manifolds $W^s_{P_{1,2}}$ do not intersect the switching line between A and E. Choose a horizontal slab H_1 along the stable manifold $W^s_{P_2}$ from P_2 until $W^u_{P_1}$ to satisfy the following conditions. For a suitable integer $k > 1$, $f^{k-1}(H_1)$ must lie above the switching line such that it contains B and a point between P_2 and A on $W^u_{P_2}$. Then $V_1 := f^k(H_1)$ contains C and fully intersects H_1. The thickness of V_1 can be adjusted by an appropriate choice of k together with the vertical size of H_1. The other slab H_0 is chosen to lie along $W^u_{P_2}$ from point A to point C and be thick enough to be fully intersected by V_1. Now we can observe that $V_0 := f(H_0)$ fully intersects H_1, if D is underneath $W^s_{P_2}$. In this case we have topological conjugacy with the schematic inset of Fig. 8.b.

The calculated manifolds and the iterated sets do indeed satisfy the above condition, so we can describe the dynamics by means of the horseshoe structure of the inset, that is, by means of the left shift on the space of infinite sequences of two symbols equipped with the transition matrix

$$\begin{pmatrix} 0 & 1 \\ 1 & 1 \end{pmatrix}.$$

This matrix is irreducible [25, 13], so the motion of the system is indeed chaotic.

8 Conclusion

The non-linear analysis of highly interrupted low immersion milling shows that both the period doubling and the Neimark-Sacker bifurcations are subcritical, similar to the Hopf bifurcation results of Stépán and Kalmár Nagy [19] obtained for regenerative machine tool vibrations in case of turning. The approximate amplitudes of the unstable period-2 and quasiperiodic vibrations were also determined in closed form. These give useful estimations for the domain of attraction of stable stationary cutting in case of high-speed milling.

Also, the existence and the stability of another, global (outer) period-2 oscillation was shown and determined. In those parameter domains of cutting speed and chip width, where both the local and the global period two oscillations as well as the stationary cutting are unstable, the existence of chaotic oscillations was shown. The analytical predictions were supported and also confirmed by numerical simulations.

Although our model is very simple the results are qualitatively the same in the case of non-infinitesimal cutting time as found by simulations [2] and experiments [14]. The recent work of Stépán et *al.* [21] shows also that period

doubling bifurcations in the delay equation model are subcritical and outer period-2 orbits are connected to the unstable orbits through a fold bifurcation. A detailed analysis of period-2 orbits can be found in a forthcoming paper by the authors [22]. The demonstration of chaotic motion can be more difficult in the delay equation model because of the infinite dimensional phase space. In this case, instead of our purely geometric method of constructing the chaotic attractor one could compute 1 dimensional unstable manifolds of periodic orbits to obtain some information of the structure of chaotic attractor (for a guiding example see Green et *al.* [7]). The present and forthcoming analyses build the bridge to the experimental observations referring to chaos in manufacturing processes collected by Moon in [16].

Acknowledgements

During the preparations of this work the first author was supported by the Hungarian Eötvös scholarship. This research was also supported by the Hungarian National Science Foundation under grant no. OTKA T043368/03, and by the Research Group on Dynamics of Machines and Vehicles, Hungarian Academy of Sciences.

References

[1] Y. Altintas and E. Budak. Analytical prediction of stability lobes in milling. *Annals of the CIRP*, 44(1):357–362, 1995.

[2] B. Balachandran. Non-linear dynamics of milling process. *Transactions of the Royal Society*, 359:793–820, 2001.

[3] P. V. Bayly, J. E. Halley, B.P. Mann, and M. A. Davies. Stability of interrupted cutting by temporal finite element analysis. *ASME Journal of Manufacturing Science and Engineering*, 125(2):220–225, 2003.

[4] M. A. Davies, J. R. Pratt, B. Dutterer, and T. J. Burns. Stability prediction for low radial immersion milling. *Journal of Manufacturing Science and Engineering*, 125(1):217–225, 2002.

[5] E. J. Doedel, A. R. Champneys, T. F. Fairgrieve, Y. A. Kuznetsov, B. Sandstede, and X.-J. Wang. AUTO97: Continuation and bifurcation software for ordinary differential equations. Technical report, Department of Computer Science, Concordia University, Montreal, Canada, 1997. (Available by FTP from ftp.cs.concordia.ca in directory pub/doedel/auto).

[6] J. P. England, B. Krauskopf, and H. M. Osinga. Computing one-dimensional stable manifolds of planar maps without the inverse. *(preprint)*, 2003.

[7] K. Green, B. Krauskopf, and K. Engelborghs. Bistability and torus break-up in a semiconductor laser with phase-conjugate feedback. *Physica D*, 173:114–129, 2002.

[8] P. Guckenheimer and J. Holmes. *Nonlinear oscillations, Dynamical Systems, and Bifurcations of Vector Fields*. Springer-Verlag, New-York, 1983.

[9] J.E Halley, A. M. Helvey, and K. S. Smith W. R. Winfough. The impact of high-speed machining technology on the design and fabrication of aerospace components. In *Proceedings of the ASME 1999 Design Engineering Technical Conferences, Las Vegas, Nevada*, September 1999. Paper number DETC99/VIB-8057 (CD-ROM).

[10] T. Insperger, B. P. Mann, G. Stépán, and P. V. Bayly. Stability of up-milling and down-milling, part 1: alternative analytical methods. *International Journal of Machine Tool & Manufacture*, 43(1):25–34, 2003.

[11] T. Insperger and G. Stépán. Vibration frequencies in high-speed milling process or a positive answer to davies, pratt, dutterer and burns. *Journal of Manufacturing Science and Engineering*, (in press).

[12] T. Kalmár-Nagy, G. Stépán, and F. C. Moon. Subcritical hopf bifurcation in the delay equation model for machine tool vibrations. *Nonlinear Dynamics*, 26:121–142, 2001.

[13] M. Lind and B. Marcus. *An introduction to Symbolic Dynamics and Coding*. Cambridge University Press, Cambridge, 1995.

[14] B. P. Mann, T.Insperger, P. V. Bayly, and G. Stépán. Stability of up-milling and down-milling, part 2: experimental verification. *International Journal of Machine Tool & Manufacture*, 43:35–40, 2003.

[15] I. Minis and R. Yanushewsky. A new theoretical approach for the prediction of machine tool chatter in milling. *ASME Journal of Engineering for Industry*, 115:1–8, 1993.

[16] F. C. Moon. *Dynamics an Chaos in Manufacturing Processes*. Wiley, New York, 1998.

[17] J. Moser. *Stable and Random Motions in Dynamical Systems*. Princeton University Press, Princeton, 1973.

[18] H. M. Shi and S. A. Tobias. Theory of finite amplitude machine tool instability. *Int. J. Machine Tool Design and Research*, 24:45–69, 1984.

[19] G. Stépán and T. Kalmár-Nagy. Nonlinear regenerative machine tool vibrations. In *Proceedings of the 1997 ASME Design Engineering Technical Conferences, Sacramento, California*, September 1997. Paper number DETC97/VIB-4021.

[20] G. Stépán, R. Szalai, and T. Insperger. Stability of high-speed milling. In Günther Radons, editor, *Nonlinear Dynamics of Production Systems*, pages 111–128. Wiley VCH, 2003.

[21] G. Stépán, R. Szalai, B. P. Mann, P. V. Bayly, T. Insperger, J. Gradisek, and E. Govekar. Nonlinear dynamics of high-speed milling – analysis, numerics and experiments. *ASME Journal of Vibrations and Acoustics*, (in press).

[22] R. Szalai, G. Stépán, and S. J. Hogan. Continuation of bifurcations in periodic DDEs using characteristic matrices. (in preparation).

[23] J. Tlusty. *Manufacturing Process and Equipment*. Prentice Hall, New Jersey, 2000.

[24] S. A. Tobias. *Schwingungen an Werkzeugmaschinen*. Carl Hanser Verlag, München, 1961.

[25] S. Wiggins. *Global bifurcations and chaos*. Springer-Verlag, New-York, 1988.

List of Figures